Cellular Instabilities and Laminar Burning Velocities of Spherically Expanding H_2/air flames doped with methane and diluted with water

Pascal DIÉVART[1,2], Atsushi ZEMBA[3], Ayan MOUSSE-RAYALEH[1,2], Toshiyuki KATSUMI[3], Nabiha CHAUMEIX[1]
[1]ICARE-CNRS, Orléans, Loiret, France
[2]Université d'Orléans, Orléans, Loiret, France
[3]Nagaoka University of Technology, Nagaoka, Niigata, Japan

1 Introduction

Hydrogen safety in nuclear power plants is a critical aspect of ensuring the safe and efficient operation of these facilities. Indeed, hydrogen can be released during an incident by the reaction of the nuclear combustible cladding (usually made of zirconium) with water steam, resulting in an accumulation of hydrogen inside the reactor building. To prevent the ignition of the hydrogen/air mixtures, venting systems can be installed to maintain the hydrogen concentration below the lower flammability limit and water can be sprinkled to cool down the gases and slow down the combustion in case of ignition.

However, hydrogen may not be the only fuel produced during a nuclear incident. Electric wire sheaths, that run throughout the reactor building, may decompose when expose to high temperatures, producing hydrocarbon fuels that may modify the combustion and explosive properties of the hydrogen/air/water mixtures. Actually, during the nuclear accident at the Fukushima Daiichi power plant, a luminous flame was recorded by the TV cameras [1] indicating the formation of soot particles during the hydrogen explosion, and thus the presence of gas phase hydrocarbon fuels in the building.

Therefore, it is crucial to understand how small amounts of hydrocarbon fuels affect the combustion of hydrogen/air mixtures with and without water dilution. The aim of this work is to investigate experimentally the propagation of the laminar flames of hydrogen/air mixtures (10 to 20% H_2) doped with methane, considered herein as a hydrocarbon fuel surrogate, with and without water dilution. The effect of the mixture composition on the laminar flame speed, the Markstein length and the critical Peclet number is quantified and analyzed.

2 Experimental set-up

The experiments are conducted using a spherical bomb facility developed at ICARE, Orléans. This experimental setup has been thoroughly described in a previous publication [2], therefore a brief overview is hereafter given. The vessel consists of a 96-L spherical stainless-steel vessel equipped with

Correspondence to: pascal.dievart@cnrs-orleans.fr

up to 4 sapphire windows (200 mm optical diameter). The temperature inside the vessel is maintained at the desired temperature thanks to a heat transfer fluid. The uniformity of the temperature, which is measured by a K-type thermocouple, is guaranteed by a thermal insulation, resulting in a maximum deviation from the target value of at most 1 K. Prior to each experiment, the chamber is pumped down to less than 2 Pa. The gases are introduced directly into the vessel using the partial pressure approach. Steam is obtained by collecting the water vapor from a water flask located in a heating bath. Pressures during the mixture preparation are monitored using two capacitive manometers (MKS Baratron, type 631, accuracy 0.2%, 0-100 Torrs; MKS Baratron Type AA06A, accuracy 0.05%,0-15 000 Torrs). From the precision of the capacitive manometers, the uncertainties on the molar fractions are around 1%. The mixture homogeneity is ensured by activating eight fans at a speed of 1000 rpm for two minutes. After resting for five minutes, the mixture is then ignited with two tungsten electrodes located along the sphere diameter. These electrodes are connected to a regulated high voltage discharge system, which generates a spark in the center of the vessel. The voltage and the intensity of the discharge are measured using a high voltage and a current probe, enabling the calculation of the energy delivered to the mixture.

Gases were purchased from Air Liquide (Hydrogen, purity 99.999%; methane, purity 99.9999%; Air Alpha 2, O_2 20.9%, N_2 79.1%). Deionized water was used for steam generation.

The combustion is monitored using two complementary diagnostics: pressure measurements with a piezo-electric pressure transducer (Kistler 601A coupled to a Kistler Type 5018 Charge Amplifier), and visualization and recording of the expanding flames using a Z-type Schlieren coupled with a high-speed camera (Phantom TMX 5010, up to 45 000 frames per second acquisition rate). The synchronization of the two diagnostics, required in order to link the pressure rise with the data acquired by rapid imaging, is obtained by a TTL signal generated at the onset of the spark between the electrodes. The pressure signal, in particular, is utilized to ensure that all measurements were taken under constant pressure conditions.

The recorded images are then processed in order to extract the flame radius as a function of the time with an in-house software based on the Canny method. The adiabatic unstretched gas velocity of the burned gases relative to the flame, V_S^0, and the burned Markstein length, L_b, can be derived by solving either the linear equation or the non-linear equation [3] that relates the measured flame speeds V_S to the stretch rate κ.

$$V_S = V_S^0 - L_b\kappa$$

$$\left(\frac{V_S}{V_S^0}\right)^2 \ln\left(\frac{V_S}{V_S^0}\right)^2 = -\frac{2L_b\kappa}{V_S^0}$$

The unburned laminar flame speed S_L^0 and Markstein length L_u are then calculated from the continuity equations $\rho_u S_L^0 = \rho_b V_S^0$ and $\rho_u L_u = \rho_b L_b$, where ρ_u and ρ_b are the densities of the fresh and burned gases calculated with Cantera [4].

3 Results

The effect of methane doping on the propagation of a hydrogen/air flame (15% H_2) with 10% steam dilution is displayed in Figure 1. It is evident that, even in small amount, methane doping increases significantly the flame velocity. From linear extrapolation, the unstretched laminar flame speed S_L^0 increases by a factor 2, from ~25 cm/s to ~52 cm/s when adding 2% (of the total fuel/air mixture) of methane in the conditions of Figure 1. The observed increase is even higher when considering the non-linear extrapolated values (factor 2.7, from 18 to 48 cm/s).

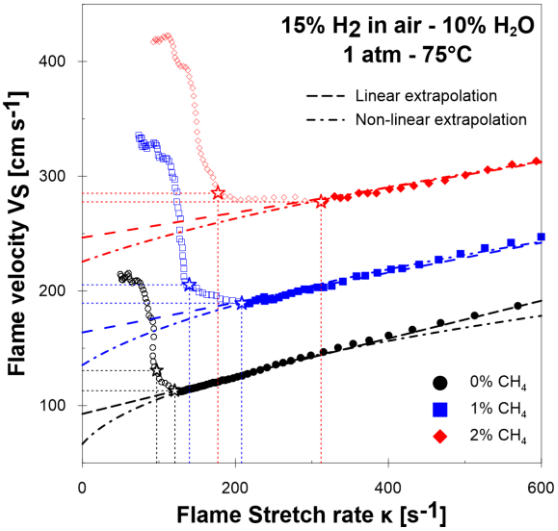

Figure 1: Flame speed as a function of flame stretch rate for H_2/air mixtures (75°C, 760 Torr and 15% of H_2 in air) doped with different amounts of methane. The closed symbols depict the data used in the zero-stretch flame velocity extrapolation. The star-shape symbols show the critical points.

Methane doping also impacts the flame radius at which hydrodynamics and thermo-diffusive instabilities occur. Those instabilities result in the wrinkling of the flame surface and a self-acceleration of the front flame displacement, therefore in a sudden change of slope in the (κ, V_S) diagram. According to Figure 1, two critical radii can be identified in the early stage of the flame. The first critical point, with an associated radius R_{cr1}, is characterized by a small change in the slope and Schlieren flame images do not show significant perturbation of the flame surface. The second critical point, with the associated radius R_{cr2}, is related to a sharp increase in the flame propagation speed and the appearance of wrinkles on the Schlieren images.

In the present work, three parameters have been varied independently: the hydrogen mole fraction in air (10, 15 and 20%), the methane mole fraction (0, 1 and 2%) and the water dilution level (0 and 10%). The direct comparison of the experimentally determined critical radius is then difficult, the use of normalized or adimensional quantities is desired. A proper substitute to the critical radius is the critical Peclet number Pe_{cr}, which is obtained by normalizing the critical radius by the laminar flame thickness δ_f. This latter is calculated according to the gradient theory as $\delta_f=(T_b-Tu)/(\partial T/\partial x)_{max}$, where T_u and T_b are unburned and burned gases temperatures and $(\partial T/\partial x)_{max}$ the maximum temperature gradient in the front flame from a 1D-flame propagation simulation. To encompass the mixture properties, Kim et al. [5] and Morsy and Yang [6] have suggested to adopt the Markstein number Ma. The Markstein number can easily be derived by normalizing the experimentally determined Marskstein length L_u by the laminar flame thickness. Additionnally, Ma can also be calculated theoretically using the relations derived by Bechtold and Matalon [7] from asymptotic theory analysis.

$$Ma_u = \frac{2}{\sqrt{\sigma}+1} + \frac{2\beta}{\sigma-1}\left(Le_{eff}-1\right)\left(\sqrt{\sigma}-1-\ln\frac{\sqrt{\sigma}+1}{2}\right)$$

where σ is the expansion factor, Le_{eff} the effective Lewis number of the reactive mixture and β the Zeldovich number. The effective Lewis number of the reactive mixture is calculated according to the expression proposed by Addabbo et al. (here applied to lean mixtures) [8]:

$$Le_{eff} = 1 + \frac{\left(Le_{O_2}-1\right)+\left(Le_{fuel}-1\right)\times A}{1+A}$$

where A is defined as $1+\beta(\varphi-1)/\varphi$ and φ the equivalence ratio. For fuel binary mixtures, Le_{fuel} is taken as the volume-based average of the individual fuel Lewis numbers as recommended by Bouvet et

al. [9] The Zeldovich number requires the calculation of the mixture activation energy, which can be achieved either using the ignition method [10] (from the derivatives of the logarithm of the ignition delay time with respect to the initial temperature at constant pressure and with respect to the mixture density at constant temperature) or the flame theory [11] (from the derivative of the logarithm of the mass burning rate with respect to the inverse of the adiabatic temperature). Both methods have been employed in this study.

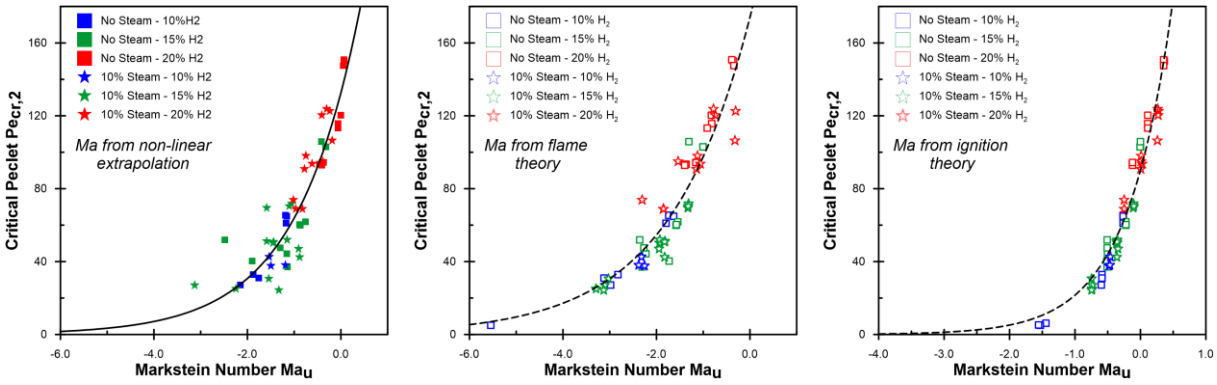

Figure 2: Second Critical Peclet number Pe_{cr2} as a function of the Markstein number for the H_2/air/CH_4/H_2O mixtures herein investigated. The lines are the best fit on the data. Theoretical calculations (Ma and δ_f) have been performed with the FFCM-2 [12]

Figure 2 displays the dependence of the second critical Peclet number to the unburned Markstein number obtained from the non-linear extrapolation of the experimental (κ, V_S) set of data and theoretical calculations using the FFCM-2 reaction mechanism [12] . A non-linear relationship is observed between the two numbers despite the small variation (from -3.2 to 0.1) of Ma across the mixtures investigated. The following correlation $Pe = 133\ e^{0.73Ma}$ is obtained on this interval with a R^2 values of 0.88. Although not displayed in Figure 2, a similar analysis can be performed using the Markstein number obtained from the linear extrapolations. In that case, the Markstein number is limited to an even smaller interval (from -0.6 to 0.0) and a linear relationship is observed ($Pe = 188\ Ma + 141$, $R^2 = 0.74$). Also shown in Figure 2 are the dependence of the second critical Peclet number to the theoretically calculated Ma. Again, a non-linear relationship is observed. It is noteworthy that the use of the flame theory activation energies leads to Ma_u, and thus a relationship ($Pe = 174\ e^{0.58Ma}$), very similar to the one obtained from the non-linearly extrapolated L_u whereas the ignition theory is more consistent with the linearly extrapolated values. These correlation enables predicting the flame size for which cellular instabilities will overtake the combustion chemistry in controlling the flame propagation.

According to the equations of Bechtold and Matalon [7], the Markstein number is a function of the effective Lewis number Le_{eff}. Therefore, from the observations of Figure 2, one could expect the critical Peclet number to be related to the Le_{eff}. Figure 3 presents the relationship between these two quantities. The critical Peclet number is observed to be linearly related to the effective Lewis number, regardless of the methodology employed in the calculation of the activation energy.

The unstretched laminar flame speeds S_L^0 determined experimentally for the 15% and 20% H_2 mixtures, with and without steam dilution, are shown in Figure 4. The mixtures herein investigated are characterized by values of $Ma_{Linear}Ka_{middle}$ close to -0.20, which was reported by Wu et al. [13] to be associated to large uncertainties in the extrapolation procedure and an overestimation of the zero-stretch flame velocity, especially with the linear-stretch model. Indeed, with the exception of the undiluted 20% H_2 conditions, the non-linear extrapolated flame speeds are consistently lower than the linear extrapolated values by up to 30%. Therefore, only the non-linear model extrapolated are displayed in Figure 4.

As mentioned earlier, methane doping results in an increase of S_L^0. In the present conditions, this increase is linear, less significant for the higher hydrogen concentration, and mitigated by steam dilution. One can observe for example that the addition of 2% methane cancels out the inhibiting effect of the 10% steam dilution for the 15% H_2 mixture.

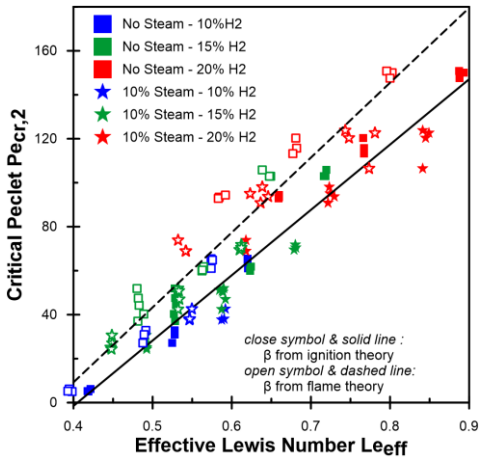

Figure 3: Second Critical Peclet number Pe_{cr2} as a function of the effective Lewis number (close symbol: Zeldovich number from ignition theory; open symbol: Zeldovich number from flame theory) for the H_2/air/CH_4/H_2O mixtures herein investigated.

The adiabatic laminar flame speeds computed by three kinetic models from the literature, namely FFCM-2 [12], NUIG 1.3 [14], and San Diego 2016 [15], are also displayed in Figure 4. These models all capture qualitatively and quantitatively the experimental measurements and observations, i.e. the linear increase in S_L^0 due to methane doping and the mitigation by steam dilution. Nonetheless, the San Diego mechanism exhibits the overall best performances, whereas the NUIG model computes the lowest flame speeds.

Because of the large water concentration, radiative effects may play a substantial role in the heat transfer from the burned gases to the fresh gases. Preliminary calculations with the optically thin model (considering only CO_2 and H_2O in Cantera) in which emissivity coefficients of the gases, calculated according to Alberti et al. [16], are specified have been performed and show that the computed laminar flame speed increases by about 10% for the steam diluted mixtures.

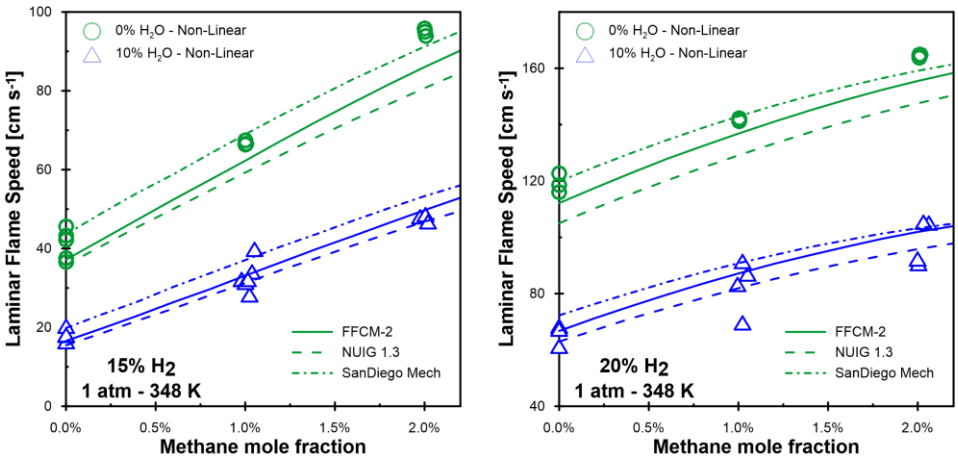

Figure 4: Adiabatic laminar burning velocities of H_2/air flames doped with different amounts of methane, with and without water dilution. Experimental values are obtained from non-linear. Solid, short- and long dashed are the values computed with the models FFCM-2 [12], NUIG 1.3 *[14]*, and San Diego 2016 *[15]*, respectively.

Conclusion

Expanding spherical flames of H_2/air mixtures doped with methane and/or diluted with steam have been studied experimentally by Schlieren imaging. Laminar burning velocities and Markstein lengths were derived from experimental measurements of radius versus time. The onset of cellular instabilities was also characterized by the determination of a critical Peclet number, which was found to be correlated to the unburned Markstein number and the effective Lewis number of the mixture through a non-linear and a linear relationship, respectively. Several recent kinetic models were also successfully tested against the experimental measurements. However, further work is required to understand and model correctly the radiative heat transfer. Additional efforts to extend the range of experimental conditions (methane amount, dilution level, temperature and pressure) shall be performed to consolidate the present conclusions. Moreover, substitution of methane with other hydrocarbon fuels, the combustion chemistry of which is more representative of the hydrocarbon fuels that may be produced during a nuclear incident, is to be considered.

References

[1] The Tokyo Electric Power Company, Inc. Fukushima Nuclear Accident Analysis Report (Interim Report). 2011.
[2] Goulier J, Chaumeix N, Halter F, Meynet N, Bentaïb A. Experimental study of laminar and turbulent flame speed of a spherical flame in a fan-stirred closed vessel for hydrogen safety application. Nuclear Engineering and Design 2017;312:214–27.
[3] Ronney PD, Sivashinsky GI. A Theoretical Study of Propagation and Extinction of Nonsteady Spherical Flame Fronts. SIAM J Appl Math 1989;49:1029–46.
[4] Goodwin DG, Moffat HK, Schoegl I, Speth RL, Weber BW. Cantera: An Object-oriented Software Toolkit for Chemical Kinetics, Thermodynamics, and Transport Processes. Zenodo; 2023.
[5] Kim W, Sato Y, Johzaki T, Endo T, Shimokuri D, Miyoshi A. Experimental study on self-acceleration in expanding spherical hydrogen-air flames. International Journal of Hydrogen Energy 2018;43:12556–64.
[6] Morsy ME, Yang J. The instability of laminar methane/hydrogen/air flames: Correlation between small and large-scale explosions. International Journal of Hydrogen Energy 2022;47:29959–70.
[7] Bechtold JK, Matalon M. The dependence of the Markstein length on stoichiometry. Combustion and Flame 2001;127:1906–13.
[8] Addabbo R, Bechtold JK, Matalon M. Wrinkling of spherically expanding flames. Proceedings of the Combustion Institute 2002;29:1527–35.
[9] Bouvet N, Halter F, Chauveau C, Yoon Y. On the effective Lewis number formulations for lean hydrogen/hydrocarbon/air mixtures. International Journal of Hydrogen Energy 2013;38:5949–60.
[10] Bane SPM. Spark Ignition: Experimental and Numerical Investigation With Application to Aviation Safety. California Institute of Technology, 2010.
[11] Ravi S, Sikes TG, Morones A, Keesee CL, Petersen EL. Comparative study on the laminar flame speed enhancement of methane with ethane and ethylene addition. Proceedings of the Combustion Institute 2015;35:679–86.
[12] Zhang Y, Dong W, Vandewalle LA, Xu R, Smith GregoryP, Wang H. Foundational Fuel Chemistry Model Version 2.0 (FFCM-2) 2023. https://web.stanford.edu/group/haiwanglab/FFCM2.
[13] Wu F, Liang W, Chen Z, Ju Y, Law CK. Uncertainty in stretch extrapolation of laminar flame speed from expanding spherical flames. Proceedings of the Combustion Institute 2015;35:663–70..
[14] Zhu L, Panigrahy S, Elliott SN, Klippenstein SJ, Baigmohammadi M, Mohamed AAE-S, et al. A wide range experimental study and further development of a kinetic model describing propane oxidation. Combustion and Flame 2023;248:112562.
[15] Williams FA. Chemical-kinetic mechanisms for combustion applications 2016. https://web.eng.ucsd.edu/mae/groups/combustion/mechanism.html (accessed January 3, 2025).
[16] Alberti M, Weber R, Mancini M. Gray gas emissivities and absorptivities for $H_2O/CO_2/CO/N_2$ mixtures. Journal of Quantitative Spectroscopy and Radiative Transfer 2024;322:109016.